Postthymic maturation influences the CD8 T cell response to antigen

Lydia E. Makaroff, Deborah W. Hendricks, Rachel E. Niec, and Pamela J. Fink[1]

Department of Immunology, University of Washington, Campus Box 357650, Seattle, WA 98195-7650

Edited by Philippa Marrack, National Jewish Medical and Research Center, Denver, CO, and approved February 6, 2009 (received for review December 4, 2008)

Complete T cell development requires postthymic maturation, and we investigated the influence of this ontological period on the CD8 T cell response to infection by comparing responses of mature CD8 T cells with those of recent thymic emigrants (RTEs). When activated with a noninflammatory stimulus or a bacterial or viral pathogen, CD8 RTEs generated a lower proportion of cytokine-producing effector cells and long-lived memory precursors compared with their mature counterparts. Although peripheral T cell maturation is complete within several weeks after thymic egress, RTE-derived memory cells continued to express inappropriate levels of memory cell markers and display an altered pattern of cytokine production, even 8 weeks after infection. When rechallenged, RTE-derived memory cells generated secondary effector cells that were phenotypically and functionally equivalent to those generated by their mature counterparts. The defects at the effector and memory stages were not associated with differences in the expression of T cell receptor-, costimulation-, or activation-associated cell surface markers yet were associated with lower Ly6C expression levels at the effector stage. This work demonstrates that the stage of postthymic maturation influences cell fate decisions and cytokine profiles of stimulated CD8 T cells, with repercussions that are apparent long after cells have progressed from the RTE compartment.

memory T cells | recent thymic emigrants

The mammalian immune system relies on long-lived memory CD4 and CD8 T cells to protect the host from recurrent bacterial or viral infections. During the primary response, the peak expansion of effector T cells that function immediately to clear the pathogen occurs at 5–8 days after infection, after which a dramatic contraction of the effector T cell compartment occurs, leaving behind a small number of antigen-specific memory T cells. These long-lived memory cells display distinct mRNA expression profiles and cell surface markers, have a wide tissue distribution, occur at higher frequencies than their naïve counterparts, and rapidly reactivate upon reencountering antigen (1–3). The factors that control the balance between the differentiation of CD8 T cells into effector versus memory cells are incompletely understood. Two of the model pathogens used to dissect the immune response in the mouse are the bacterium *Listeria monocytogenes* engineered to secrete chicken ovalbumin (Lm-OVA) and the Armstrong strain of lymphocytic choriomeningitis virus (LCMV). The effector T cells that respond to these pathogens can be subdivided in terms of cytokine profile and expression of the high-affinity IL-7 receptor α chain (CD127) and killer cell lectin-like receptor G1 (KLRG1). After infection with these pathogens, some antigen-reactive T cells multiply to become short-lived effector cells that produce IFN-γ and TNF-α, but not IL-2, and are CD127$^-$ KLRG1$^+$ (3). A smaller proportion of effector cells become long-lived memory precursor cells, often producing IL-2 (4) and exhibiting a CD127$^+$ KLRG1$^-$ phenotype. Some of the factors that influence the balance between short-lived effector cells and long-lived memory precursors have been elucidated. The duration of antigen exposure and inflammation, extent of IL-12, IFN-γ, IFN-α, and IL-2 exposure, and presence of CD4 helper T cells all influence CD8 T cell fate decisions (1–3). An additional but untested factor that may impact effector T cell fate decisions is the time that the T cell has spent maturing in the periphery after its egress from the thymus, before it meets antigen.

The pool of peripheral T lymphocytes is maintained by a combination of homeostasis and the arrival from the thymus of newly minted T cells, termed recent thymic emigrants (RTEs). It was previously technically difficult to study whether these RTEs differ from mature naïve (MN) T cells because there is no reliable cell surface marker to distinguish these two T cell subsets. Transgenic (Tg) mice that express green fluorescent protein (GFP) under the recombination activating gene (RAG) 2 promoter (5) allow the easy separation of RTEs and MN T cells from unmanipulated mice (6). After RAG2 expression is extinguished, the GFP decays gradually as the T cells mature (7), permitting the isolation of untouched live RTEs for analysis. Recent work has shown that RTEs are phenotypically and functionally immature compared with MN T cells and that peripheral maturation occurs progressively and requires T cell contact with secondary lymphoid organs (6, 8, 9).

It is unknown how RTEs interpret the signals that influence effector versus memory cell fate decisions during the early stages of infection. To address this question, we transferred into naïve hosts sorted populations of RTEs and MN T cells bearing a uniform TCR, thus ensuring that any discrepancies between MN cells and RTEs were not caused by polyclonal repertoire differences. The transferred cells were activated in situ with cognate antigen-expressing splenocytes or pathogens, revealing that effector and memory cells derived from RTEs exhibit an altered pattern of CD127 and KLRG1 expression and a decreased proportion of cytokine-producing cells. These differences were observed on two TCR Tg backgrounds in response to a noninflammatory stimulus and bacterial and viral infections. These data indicate that the postthymic maturational status of a peripheral T cell influences the fate decisions that cell will make in response to antigen.

Results

RTEs Produce a Lower Proportion of Long-Lived Memory Precursors and Cytokine-Producing Cells When Activated with a Noninflammatory Stimulus. Congenically marked RTEs and MN cells from OT-1 Tg mice (expressing a uniform MHC class I-restricted OVA-specific TCR) were isolated and coinjected into hosts that subsequently received cells expressing membrane-bound OVA under the actin promoter (Act-mOVA), a noninflammatory stimulus (Fig. 1 *A*). This regimen results in a modest expansion of transferred cells with a peak of OVA-specific cytokine response occurring 10 days after antigen inoculation (10, 11).

Author contributions: L.E.M. and P.J.F. designed research; L.E.M., D.W.H., and R.E.N. performed research; L.E.M., D.W.H., R.E.N., and P.J.F. analyzed data; and L.E.M. and P.J.F. wrote the paper.

The authors declare no conflict of interest.

This article is a PNAS Direct Submission.

[1]To whom correspondence should be addressed. E-mail: pfink@u.washington.edu.

IMMUNOLOGY

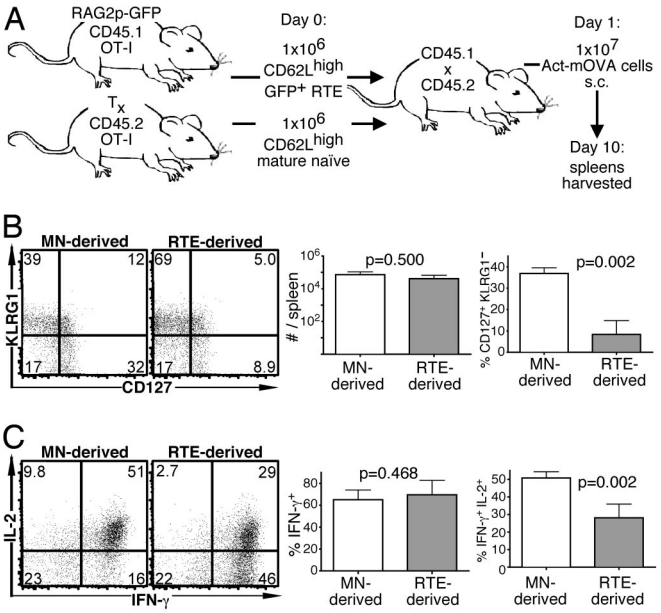

Fig. 1. Compared with MN cells, RTEs produce a distinct effector response to a noninflammatory stimulus. (*A*) Experimental setup. (*B*) Representative plots of CD127 and KLRG1 expression by transferred donor cells and mean total number of donor cells and percentage of CD127$^+$ KLRG1$^-$ donor cells from 4 recipients. (*C*) Representative intracellular IL-2 and IFN-γ production by donor cells from recipient spleens after a 5-h peptide restimulation and mean percentage of IFN-γ$^+$ and IFN-γ$^+$ IL-2$^+$ cells. Bars represent standard deviations from the mean. The indicated *P* values were calculated by using two-tailed Student's *t* tests with equal variance. T_x, thymectomized.

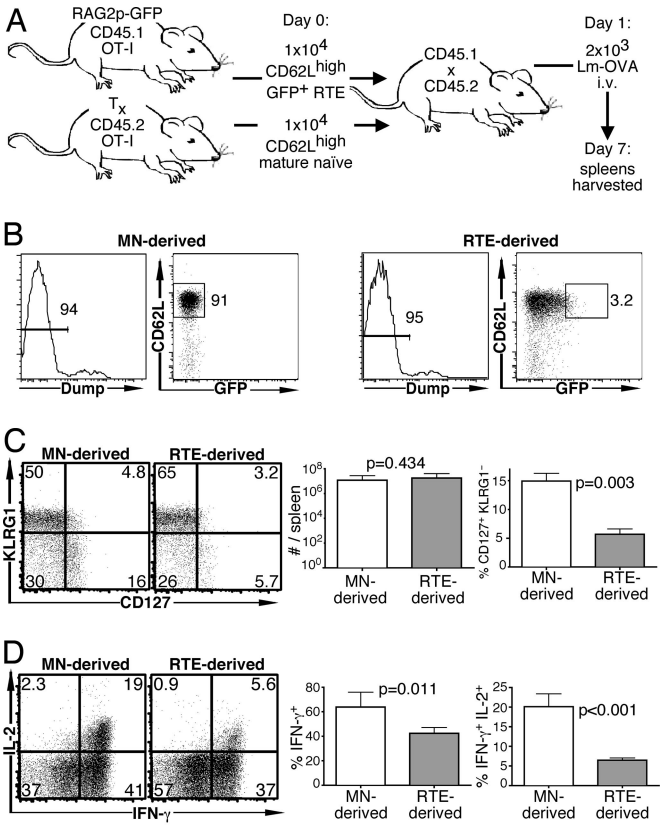

Fig. 2. Compared with MN cells, RTEs generate fewer memory precursor cells in response to bacterial infection. (*A*) Experimental setup. (*B*) Representative sorting gates showing the strategy used to isolate OT-1 Tg RTEs and MN T cells from bead-depleted populations. Cells expressing CD4, NK1.1, CD11b, B220, or Ter-119 (dump$^+$) were excluded, and dump$^-$ cells were further selected for expression of CD62L (for both RTEs and MN T cells) and GFP (for RTEs). Approximately 3% of the brightest GFP$^+$ cells were used as the source of RTEs, representing the newest emigrants. (*C*) Representative plots of CD127 and KLRG1 expression by transferred donor cells and mean total number of donor cells and percentage of CD127$^+$ KLRG1$^-$ donor cells from a total of 4–8 recipients. (*D*) Representative intracellular IL-2 and IFN-γ production by donor cells from recipient spleens after a 5-h peptide restimulation and mean percentage of IFN-γ$^+$ and IFN-γ$^+$ IL-2$^+$ cells. Bars represent standard deviations from the mean. The indicated *P* values were calculated by using two-tailed Student's *t* tests with equal variance.

There was no significant difference in the number of RTE- and MN-derived OT-1 CD8 T cells 10 days after injection of OVA-expressing cells (Fig. 1*B*), and previous work has shown that the initial survival of adoptively transferred RTEs and MN cells is the same (9). However, the cells derived from RTEs were phenotypically distinct because a significantly lower proportion of the population was CD127$^+$ KLRG1$^-$ (Fig. 1*B*). Although the proportion of IFN-γ-producing cells did not differ between these two populations, the mean fluorescence intensity of IFN-γ$^+$ cells was lower in the RTE-derived (17,615 ± 1,023 units) than in the MN-derived population (19,814 ± 1,023 units, $P = 0.0464$). In addition, compared with MN-derived cells, a lower proportion of RTE-derived cells produced IL-2 (Fig. 1*C*). Thus, when RTEs encounter antigen before completing peripheral maturation, their effector progeny are functionally distinct from those produced by MN cells.

Effector and Memory Cells Derived from RTEs Produce a Distinct Response to Bacterial Infection. It was of interest to investigate the characteristics of memory cells derived from RTEs by using an infectious model. In an experimental setup similar to that used above, congenically marked RTEs and MN cells from OT-1 Tg mice were coinjected into hosts that were subsequently infected with Lm-OVA (Fig. 2*A*). Both cell types (identified by CD45 allele expression and confirmed by OVA-specific tetramer staining) expanded in response to the infection, and at 7 days there was no significant difference in the number of RTE- and MN-derived OT-1 T cells. A lower proportion of the RTE-derived population was CD127$^+$ KLRG1$^-$ (Fig. 2*C*), suggesting a defect in generating competent memory cell precursors. Furthermore, compared with MN-derived cells, a significantly lower proportion of RTE-derived cells produced the cytokines IFN-γ and IL-2 (Fig. 2*D*). Of those RTE-derived cells that were IFN-γ$^+$ IL-2$^+$, the mean fluorescence intensity of IL-2 staining was significantly lower than that of their MN-derived counterparts (1,541 ± 79 units versus 2,262 ± 198 units, $P < 0.001$).

Memory cells were investigated 60 days after Lm-OVA infection, and there was no significant difference in the number of RTE- and MN-derived OT-1 T cells. However, the properties of the RTE-derived memory cells were markedly impaired compared with their MN-derived counterparts. The RTE-derived memory cells displayed aberrant levels of CD127 and KLRG1 (Fig. 3*A*), and a lower proportion produced IL-2 (Fig. 3*B*), whereas the proportion of cells that were IFN-γ-positive was not different (Fig. 3*B*). Thus, the functional impairments displayed by RTE-derived effectors are still apparent in memory cells >8 weeks after primary infection. These distinct properties were not associated with differences in basal turnover because a similar proportion of memory cells from both cell populations incorporated BrdU over 8 days (Fig. 3*C*). Three and 5 days after rechallenge with a higher dose of Lm-OVA, there were no significant differences in the properties of secondary effector OT-1 CD8 cells derived from RTEs and MN T cells (Fig. 4).

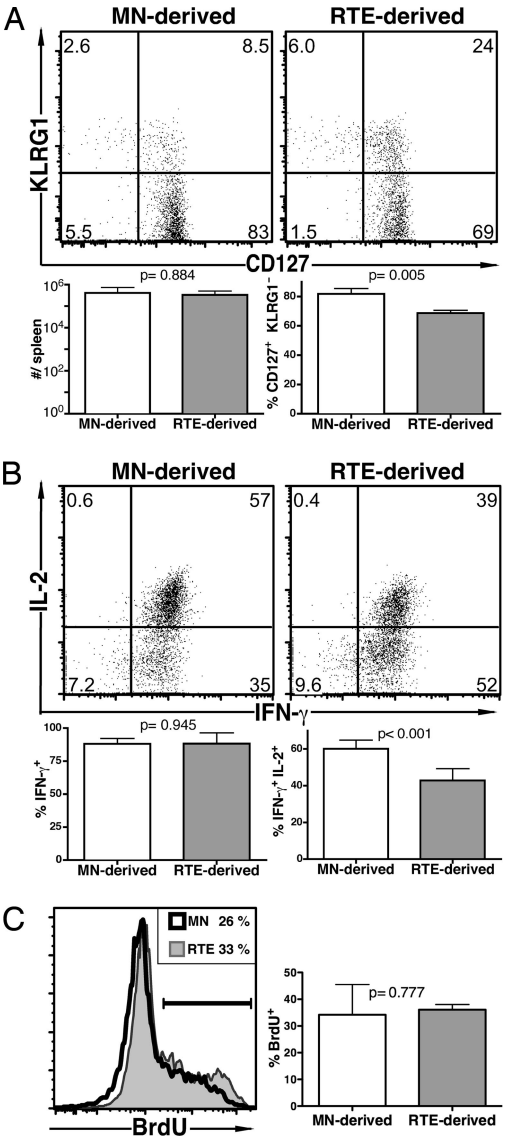

Fig. 3. In response to a bacterial pathogen, a lower proportion of RTE-derived memory cells produce IL-2 than their MN-derived counterparts. The experiment was designed as in Fig. 2; however, mice were killed at day 60. (*A*) Representative plots of CD127 and KLRG1 expression by transferred donor cells and mean total number of donor cells and percentage of CD127$^+$ KLRG1$^-$ donor cells from a total of 4–6 recipients. (*B*) Representative intracellular IL-2 and IFN-γ production by donor cells from recipient spleens after a 5-h peptide restimulation and mean percentage of IFN-γ^+ and IFN-γ^+ IL-2$^+$ cells. (*C*) Representative histograms of BrdU incorporation by donor cells and mean percentage of BrdU$^+$ cells from a total of 6 recipients. Bars represent standard deviations from the mean. The indicated *P* values were calculated by using two-tailed Student's *t* tests with equal variance.

The primary effector, memory, and secondary effector cells derived from RTEs and MN cells did not differ in their expression of Vα2, the signaling molecules CD5 and CD28, the activation markers CD25 and CD44, the adhesion protein CD62L, or the IL-2 and IL-15 receptor component CD122 (Fig. 5). Seven days after infection, all of the transferred cells, whether RTE- or MN-derived, were CD44^{high} and CD62L^{low}, indicating that all had undergone activation during the primary response. The RTE- and MN-derived cells also expressed indistinguishable levels of Vβ5, CD2, CD69, and ICAM. At the effector stage, a lower amount of Ly6C was present on the surface of cells derived from RTEs (Fig. 5, *Bottom*).

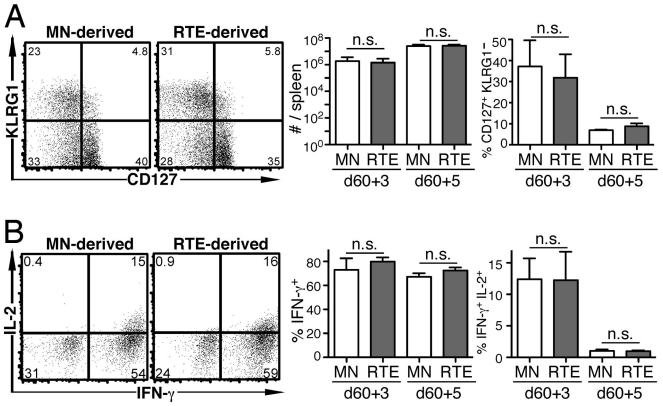

Fig. 4. RTEs are not defective in their secondary effector response to a bacterial pathogen. The experiment was designed as in Fig. 2; however, mice were rechallenged with Lm-OVA on day 60 and killed 3 or 5 days later. (*A*) Representative plots of CD127 and KLRG1 expression by transferred donor cells and mean total number of donor cells and percentage of CD127$^+$ KLRG1$^-$ cells from a total of 3–6 recipients. (*B*) Representative intracellular IL-2 and IFN-γ production by transferred donor cells after a 5-h peptide restimulation and mean percentage of IFN-γ^+ and IFN-γ^+ IL-2$^+$ cells. Bars represent standard deviations from the mean. n.s., not significant; *P* values calculated by using two-tailed Student's *t* tests with equal variance were all >0.5.

Defects in RTE-Derived Effector Cells Are Not Pathogen- or TCR-Specific. RTEs were examined further to determine their ability to protect against a viral pathogen by using the Tg P14 TCR that recognizes LCMV gp33 in the context of MHC class I molecules. At 8 days after LCMV infection of hosts containing transferred P14 Tg CD8 RTEs and MN cells (Fig. 6*A*), there was no significant difference in the number of RTE- and MN-derived cells. Similar to RTE-derived OT-1 effectors, a lower proportion of RTE-derived P14 effector cells were CD127$^+$ KLRG1$^-$ (Fig. 6*B*), and the effectors derived from RTEs included a lower proportion of IL-2 producers (Fig. 6*C*). RTE- and MN-derived effectors expressed similar levels of the cell surface markers illustrated in Fig. 5. These data demonstrate that the defects apparent in RTE-derived effectors are not restricted to a particular Tg TCR or type of infection.

Discussion

Previous work has demonstrated that CD8 T cell fate decisions are in part determined by inflammatory cytokine exposure, costimulation, the presence of CD4 helper T cells, and the duration of antigenic stimulation (1–3, 12). Asymmetric cell division may also influence the differentiation of effector and memory cell lineages, indicating that relatively minor variations in protein concentrations during stimulation can alter long-term outcomes (13). Additional factors that influence the balance between the generation of short-lived effectors and long-lived memory cells are incompletely understood. We now demonstrate that the extent of postthymic maturation influences the CD8 T cell effector versus memory cell fate balance. When a CD8 T cell that has recently left the thymus encounters antigen, it is more likely to adopt a CD127$^-$ KLRG1$^+$ terminal effector cell fate in preference to becoming an IL-2-producing CD127$^+$ KLRG1$^-$ long-lived memory precursor.

What are the potential consequences of this cell fate imbalance? Skewing the RTE response toward terminal effector cells may be important for neonatal immunocompetence. The neonatal lymphoid periphery is both lymphopenic and predominantly comprised of RTEs, one of the likely reasons that neonates display a decreased T cell-mediated memory response to most vaccines (14). Under these conditions, it is crucial to devote the few available antigen-reactive T cells to

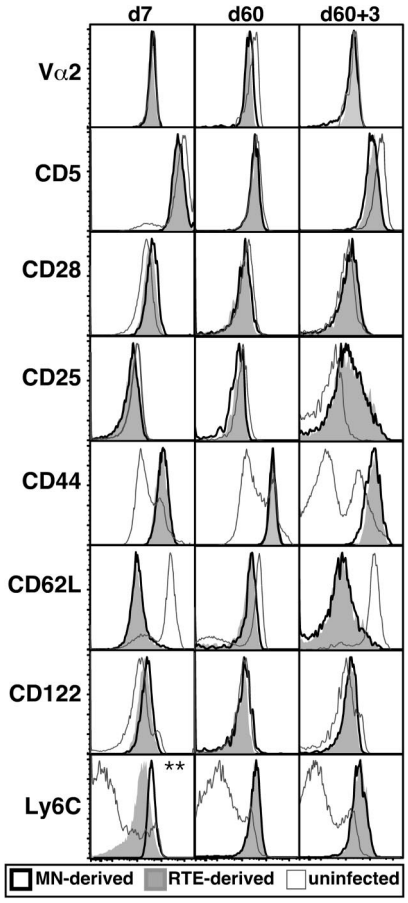

Fig. 5. RTEs express appropriate levels of TCR-related, costimulatory, and activation markers after infection, apart from lower levels of Ly6C at the effector stage. Representative histograms of the indicated surface marker expression by uninfected (open histograms with gray line), MN-derived (open histograms with bold black line), and RTE-derived (filled gray histograms) OT-1 Tg CD8 T cells, analyzed 7 days after primary Lm-OVA infection. **, $P < 0.05$, two-tailed Student's *t* test with equal variance. Data are from 3 or more independent experiments for a total of 4–10 recipients.

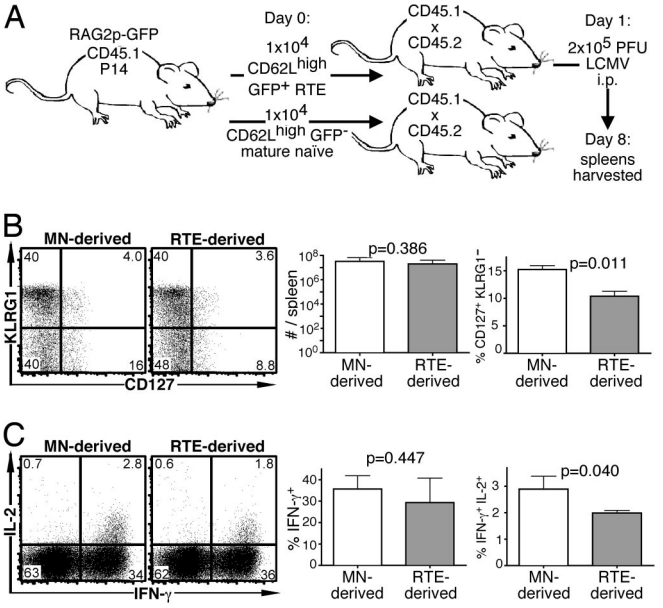

Fig. 6. RTEs are defective in their effector response to a viral pathogen. (*A*) Experimental setup. Note that both RTEs and MN T cells were sorted as dump$^-$ CD62L^{high} and GFP$^-$ (MN) or GFP$^+$ (RTEs) from the same pool of donors. (*B*) Representative plots of CD127 and KLRG1 expression by transferred donor cells and mean total number of donor cells and percentage of CD127$^+$ KLRG1$^-$ cells from a total of 4–8 recipients. (*C*) Representative intracellular IL-2 and IFN-γ production by donor cells from recipient spleens after a 5-h peptide restimulation and mean percentage of IFN-γ^+ and IFN-γ^+ IL-2$^+$ donor cells. Bars represent standard deviations from the mean. The indicated *P* values were calculated by using two-tailed Student's *t* tests with equal variance.

the effector cell pathway because in the absence of effective pathogen clearance, developing a long-lived memory population is irrelevant. However, KLRG1$^+$ cells may not protect the adult individual as well as KLRG1$^-$ cells can because of their diminished proliferative ability (15). In the adult, the CD127$^+$ KLRG1$^-$ population that produces IL-2 and serves as a reservoir of competent memory T cells (3) can be provided by the descendants of MN cells. It is interesting to note that RTEs also express less CD127 before infection (6), suggesting that this cell population has a distinct requirement for IL-7 both before and after antigen stimulation. Because altered levels of CD127 have been associated with multiple sclerosis (16), this trait may influence RTE tolerance toward self-antigens. It is clear that in the context of a heavy secondary bacterial infection, RTE-derived memory cells can compensate for their functional defects to generate a robust recall response.

In each of the antigen delivery systems we analyzed, the accumulation of RTE-derived T cells at the peak of the response was as robust as that of MN-derived cells. The absence of an apparent defect in RTE accumulation is somewhat surprising, given the proliferative defects of terminal KLRG1$^+$ cells relative to their KLRG1$^-$ counterparts (15). These results also contrast with the diminished in vivo accumulation of antigen-reactive Vβ5 TCR Tg RTE-derived T cells after Lm-OVA infection (6). In the latter case, TCR-α chain repertoire differences between RTEs and MN CD8 T cells could come into play, a variable we have eliminated in our experiments by the use of monoclonal T cell populations.

The underlying causes of the skewed effector/memory precursor cell balance among RTEs remain unclear. T-bet is one of the lineage-determining transcription factors involved in the differentiation of CD8 effectors, and in some cases it has been found to regulate the effector versus memory cell fate decision (17). This transcription factor may not be the master regulator of cell fate decisions in RTE-derived cells because no differences were seen in T-bet expression between antigen-reactive RTE- and MN-derived CD8 cells by intranuclear staining. Similarly, the differences observed between RTE- and MN-derived cells are not caused by altered levels of infection, antigen load, availability of CD4 T cell help, or cytokine milieu, given that in most of our experiments, both congenically marked cell subsets encountered antigen in the same immunocompetent host. Furthermore, our experimental design eliminated differences in TCR repertoire and idiosyncrasies caused by the analysis of a single TCR Tg line as possible contributors to the differences exhibited by RTE- and MN-derived effectors. The use of stimuli supplying little to no inflammation (OVA-expressing spleen cells), inflammation with high levels of IFNα (LCMV infection), and inflammation with high levels of IL-12 (Lm-OVA infection) further indicate that the skewed effector/memory precursor balance exhibited by RTE-derived cells is unlikely to be precipitated by differences in sensitivity to inflammatory stimuli. Furthermore, from the analysis of cell surface markers, it appears that the RTE-associated defects are not correlated with differing levels of TCR signaling, coactivation marker expression, or degree of

cellular activation. The similar levels of BrdU incorporation by RTE- and MN-derived memory cells also suggest that the distinct cytokine profiles cannot be attributed to differences in homeostatic proliferation. However, RTEs and MN T cells may differ in their trafficking, localization, or homing properties. Such differences could lead RTEs to receive more stimulation during the later stages of infection, thereby preferentially driving them toward the terminally differentiated effector cell fate (12). Of potential import in this regard is the fact that the imbalance in effector/memory precursor cell fate choice is correlated with lower surface expression of Ly6C by RTE-derived effectors. Interestingly, Ly6C is a T cell surface glycoprotein involved in cytolysis, proliferation, IL-2 and IFN-γ production, homing, and adhesion to endothelial cells (18, 19). Ly6C expression levels alone are unlikely to drive the full RTE phenotype, and we are currently undertaking a comparative array analysis of RTE- and MN-derived transcripts to search for other molecules that might influence RTE cell fate decisions.

The programming of cells to become either terminal effectors or long-lived memory cells can occur as early as 4 days after infection (12, 13, 17). Thus, the imbalance of RTE cell fate decisions may be established very early in response to stimulation. The functional impairments that characterize RTE-derived effectors are still apparent >8 weeks after primary infection, a time well exceeding the 3 weeks that RTEs require to mature fully in the periphery. Thus, T cell-intrinsic factors defined by the stage of postthymic maturation at the time of initial antigen contact can result in long-lived differences in cytokine production profiles by antigen-reactive CD8 T cells.

Experimental Procedures

Mice. RAG2p-GFP Tg mice were originally provided by M. Nussenzweig [NG-BAC mice (5)]. These mice were backcrossed in our laboratory at least 10 generations onto the C57BL/6 background and then were crossed onto the OT-1 (20) or P14 (21) Tg C57BL/6 backgrounds where indicated. The Vα2/Vβ5 OT-1 TCR binds to the SIINFEKL peptide of OVA, and the Vα2/Vβ8 P14 TCR binds to the KAVYNFATM peptide of LCMV, both presented by MHC class I. C57BL/6 mice expressing Act-mOVA (22) were obtained from M. J. Bevan (University of Washington, Seattle). Mice were thymectomized (T_x) as described in ref. 23 and used at least 3 weeks later as a source of RTE-free peripheral T cells. For in vivo BrdU incorporation studies, mice were given drinking water containing 0.8 mg/mL BrdU (Sigma–Aldrich), made fresh and changed daily for 8 days. Mice were 6–12 weeks of age at the beginning of each experiment. All experiments were carried out according to the University of Washington Institutional Animal Care and Use Committee regulations.

Flow Cytometry. Single-cell suspensions from RBC-depleted spleens were counted, and Fc receptors were blocked with anti-CD16/32 (2.4G2; BD PharMingen). Cells were stained with fluorochrome-labeled antibodies as described in ref. 24 and analyzed on a FACSCanto (Becton Dickinson) with FlowJo software (TreeStar). Dead cells were excluded on the basis of forward- and side-scatter profiles. Monoclonal antibodies were purchased from BD PharMingen, eBioscience, and Abcam and included biotinylated and FITC-, phycoerythrin- (PE), peridinin-chlorophyll-protein-Cy5.5-, PE-Cy7-, allophycocyanin- (APC), or APC-Alexa Fluor 750-conjugated antibodies specific for CD4 (RM4-5 and H129.19), CD5 (53-7.3), CD8α (53-6.7), CD25 (7D4), CD44 (IM7), CD127/IL-7Rα (A7R34), Vα2 (B20.1), CD2 (RM2-5), CD28 (37.51), CD62L (MEL-14), CD54/ICAM-1 (YN1/1.7.4), CD122/IL-2Rβ (5H4), Ly6C (HK1.4), CD45.1 (A20), CD45.2 (104), KLRG1/MAFA (2F1), T-bet (eBio4B10), and Vβ5 (MR9′4). APC-conjugated streptavidin was used in conjunction with biotinylated antibodies. Intracellular staining with APC-labeled anti-BrdU (3D4; BD PharMingen) was done according to the manufacturer's protocol. For intracellular cytokine staining, RBC-depleted splenocytes were incubated for 5 h at 37 °C with GolgiPlug (BD PharMingen) and a 10 nM concentration of the relevant OVA or LCMV peptide (both from Invitrogen). Intracellular staining with APC-labeled anti-IFN-γ (XMG1.2; BD PharMingen) and PE-labeled anti-IL-2 (JES6–5H4; eBioscience) used the Cytofix/Cytoperm kit (BD PharMingen) according to the manufacturer's protocol. For sorting, untouched CD8 T cells were enriched with an EasySep kit (StemCell Technologies) and stained to eliminate non-CD8 T cell lineages with PE-conjugated anti-CD4, anti-CD11b (M1/70), anti-NK1.1 (PK136), anti-CD45R/B220 (RA3–6B2), and anti-Ly76 (Ter-119), all from eBioscience or BD Biosciences. Cells were sorted on a FACSAria or FACSVantage (BD Biosciences) as PE$^-$ CD62L^{high} and either GFP$^+$ or GFP$^-$ to >96% purity. Cells sorted as CD62L^{high} were found to be CD44^{low} naïve T cells upon analysis.

Adoptive Transfers, Immunizations, and Infections. For Act-mOVA experiments, sorted populations of CD8 RTEs (CD45.1 GFP$^+$ CD62L^{high} cells from OT-1 Tg RAG2p-GFP Tg mice) and CD8 MN cells (CD45.2 CD62L^{high} cells from OT-1 Tg mice T_x at least 3 weeks prior) were transferred i.v. into the same CD45.1×CD45.2 hosts (1×10^6 of each cell type per mouse). One day later, recipients were injected s.c. with 1×10^7 irradiated Act-mOVA spleen and lymph node cells as described in ref. 11. Recipient spleens were harvested 10 days after priming and stained for CD4, CD8, CD45.1, and CD45.2 surface expression to identify donor cells.

Alternatively, 1×10^4 of each sorted donor cell population were transferred i.v. into CD45.1×CD45.2 hosts. Erythromycin-resistant Lm-OVA (25) was provided by M. J. Bevan and prepared as described in ref. 26. For primary infections, mice were injected i.v. with 2,000 cfu of Lm-OVA at midlog phase 1 day after adoptive transfer of donor cells. For rechallenge experiments, mice were injected i.v. with 2×10^5 cfu of Lm-OVA at midlog phase 60 days after adoptive transfer of donor cells. Spleens were harvested 7 or 60 days after primary infection and 3 or 5 days after rechallenge and stained for CD4, CD8, CD45.1, and CD45.2 surface expression to identify donor cells.

For LCMV experiments, sorted populations of CD8 RTEs (CD45.1 GFP$^+$ CD62L^{high} cells) and CD8 MN cells (CD45.1 GFP$^-$ CD62L^{high} cells) from P14 Tg RAG2p-GFP Tg mice were transferred i.v. into separate CD45.1×CD45.2 hosts (1×10^4 of each cell type per mouse). LCMV Armstrong was provided by M. K. Kaja (University of Washington, Seattle). Recipients were injected i.p. with LCMV (2×10^5 PFU per mouse) 1 day after donor cell adoptive transfer. Spleens were harvested 8 days after LCMV infection and stained for CD4, CD8, CD45.1, and CD45.2 surface expression to identify donor cells.

ACKNOWLEDGMENTS. We thank Drs. M. Nussenzweig, M. J. Bevan, and M. K. Kaja for mice and reagents and J. S. Hale for technical advice. This work was supported by National Institutes of Health Grant AI 064318 (to P.J.F. with a supplement to D.W.H.) and Medical Scientist Training Program National Institute of General Medical Sciences/National Institutes of Health Grant T32 GM007266 (to R.E.N).

1. Williams MA, Bevan MJ (2007) Effector and memory CTL differentiation. *Annu Rev Immunol* 25:171–192.
2. Harty JT, Badovinac VP (2008) Shaping and reshaping CD8$^+$ T cell memory. *Nat Rev Immunol* 8:107–119.
3. Joshi NS, Kaech SM (2008) Effector CD8 T cell development: A balancing act between memory cell potential and terminal differentiation. *J Immunol* 180:1309–1315.
4. Saparov A, et al. (1999) Interleukin-2 expression by a subpopulation of primary T cells is linked to enhanced memory/effector function. *Immunity* 11:271–280.
5. Yu W, et al. (1999) Continued RAG expression in late stages of B cell development and no apparent reinduction after immunization. *Nature* 400:682–687.
6. Boursalian TE, Golub J, Soper DM, Cooper CJ, Fink PJ (2004) Continued maturation of thymic emigrants in the periphery. *Nat Immunol* 5:418–425.
7. McCaughtry TM, Wilden MS, Hogquist KA (2007) Thymic emigration revisited. *J Exp Med* 204:2513–2520.
8. Hale JS, Boursalian TE, Turk GL, Fink PJ (2006) Thymic output in aged mice. *Proc Natl Acad Sci USA* 103:8447–8452.
9. Houston EG, Jr, Nechanitzky R, Fink PJ (2008) Cutting edge: Contact with secondary lymphoid organs drives postthymic T cell maturation. *J Immunol* 181:5213–5217.
10. Janssen EM, et al. (2005) CD4$^+$ T cell help controls CD8$^+$ T cell memory via TRAIL-mediated activation-induced cell death. *Nature* 434:88–93.
11. Sacks JA, Bevan MJ (2008) TRAIL deficiency does not rescue impaired CD8$^+$ T cell memory generated in the absence of CD4$^+$ T cell help. *J Immunol* 180:4570–4576.
12. Sarkar S, et al. (2008) Functional and genomic profiling of effector CD8 T cell subsets with distinct memory fates. *J Exp Med* 205:625–640.
13. Chang JT, et al. (2007) Asymmetric T lymphocyte division in the initiation of adaptive immune responses. *Science* 315:1687–1691.
14. Adkins B, Leclerc C, Marshall-Clarke S (2004) Neonatal adaptive immunity comes of age. *Nat Rev Immunol* 4:553–564.
15. Voehringer D, et al. (2001) Viral infections induce abundant numbers of senescent CD8 T cells. *J Immunol* 167:4838–4843.
16. Lundmark F, et al. (2007) Variation in interleukin 7 receptor α chain (IL-7R) influences risk of multiple sclerosis. *Nat Genet* 39:1108–1113.

17. Joshi NS, et al. (2007) Inflammation directs memory precursor and short-lived effector CD8$^+$ T cell fates via the graded expression of T-bet transcription factor. *Immunity* 27:281–295.
18. Walunas TL, Bruce DS, Dustin L, Loh DY, Bluestone JA (1995) Ly6C is a marker of memory CD8$^+$ T cells. *J Immunol* 155:1873–1883.
19. Jaakkola I, Merinen M, Jalkanen S, Hanninen A (2003) Ly6C induces clustering of LFA-1 (CD11a/CD18) and is involved in subtype-specific adhesion of CD8 T cells. *J Immunol* 170:1283–1290.
20. Hogquist KA, et al. (1994) T cell receptor antagonist peptides induce positive selection. *Cell* 76:17–27.
21. Pircher H, et al. (1990) Viral escape by selection of cytotoxic T cell-resistant virus variants in vivo. *Nature* 346:629–633.
22. Ehst BD, Ingulli E, Jenkins MK (2003) Development of a novel transgenic mouse for the study of interactions between CD4 and CD8 T cells during graft rejection. *Am J Trans* 3:1355–1362.
23. Boursalian TE, Bottomly K (1999) Survival of naive CD4 T cells: Roles of restricting versus selecting MHC class II and cytokine milieu. *J Immunol* 162:3795–3801.
24. Suzuki I, Martin S, Boursalian TE, Beers C, Fink PJ (2000) Fas ligand costimulates the in vivo proliferation of CD8$^+$ T cells. *J Immunol* 165:5537–5543.
25. Foulds KE, et al. (2002) Cutting edge: CD4 and CD8 T cells are intrinsically different in their proliferative responses. *J Immunol* 168:1528–1532.
26. Sun JC, Bevan MJ (2003) Defective CD8 T cell memory after acute infection without CD4 T cell help. *Science* 300:339–342.